Bacterial precursors and unsaturated long-chain fatty acids are biomarkers of North-Atlantic demosponges

Short title: Fatty acid profiles of deep-sea demosponges

Anna de Kluijver[1*], Klaas G.J. Nierop[1*], Teresa M. Morganti[2], Martijn C. Bart[3], Beate M. Slaby[4], Ulrike Hanz[5], Jasper M. de Goeij[3], Furu Mienis[5], Jack J. Middelburg[1]

[1]Department of Earth Sciences, Faculty of Geosciences, Utrecht University, Utrecht, Netherlands

[2]Max Planck Institute for Marine Microbiology, Bremen, Germany

[3]Department of Freshwater and Marine Ecology, Institute for Biodiversity and Ecosystem Dynamics, University of Amsterdam, Amsterdam, Netherlands

[4]GEOMAR Helmholtz Centre for Ocean Research Kiel, Kiel, Germany

[5]NIOZ-Royal Netherlands Institute for Sea Research and Utrecht University, Den Burg, Texel, Netherlands.

*corresponding authors

Email: a.dekluijver@uu.nl; k.g.j.nierop@uu.nl

Abstract

Sponges produce distinct fatty acids (FAs) that (potentially) can be used as chemotaxonomic and ecological biomarkers to study endosymbiont-host interactions and the functional ecology of sponges. Here, we present FA profiles of five common habitat-building deep-sea sponges (class Demospongiae, order Tetractinellida), which are classified as high microbial abundance (HMA) species. *Geodia hentscheli, G. parva, G. atlantica, G. barretti,* and *Stelletta rhaphidiophora* were collected from boreal and Arctic sponge grounds in the North-Atlantic Ocean. Bacterial FAs dominated in all five species and particularly isomeric mixtures of mid-chain branched FAs (MBFAs, 8- and 9-Me-$C_{16:0}$ and 10 and 11-Me-$C_{18:0}$) were found in high abundance (together ≥ 20% of total FAs) aside more common bacterial markers. In addition, the sponges produced long-chain linear, mid- and *a(i)*-branched unsaturated FAs (LCFAs) with a chain length of 24–28 C atoms and had predominantly the typical $\Delta^{5,9}$ unsaturation, although also $\Delta^{9,19}$ and (yet undescribed) $\Delta^{11,21}$ unsaturations were identified. *G. parva* and *S. rhaphidiophora* each produced distinct LCFAs, while *G. atlantica, G. barretti*, and *G. hentscheli* produced similar LCFAs, but in different ratios. The different bacterial precursors varied in carbon isotopic composition ($\delta^{13}C$), with MBFAs being more enriched compared to other bacterial (linear and *a*(*i*)-branched) FAs. We propose biosynthetic pathways for different LCFAs from their bacterial precursors, that are consistent with small isotopic differences found in LCFAs. Indeed, FA profiles of deep-sea sponges can serve as chemotaxonomic markers and support the conception that sponges acquire building blocks from their endosymbiotic bacteria.

Introduction

Sponges are abundant inhabitants of nearly all aquatic ecosystems including the deep-sea (1). They are sessile filter feeders with unique features, such as their enormous filtration capacity and their symbiosis with dense and diverse communities of (sponge-specific) microbes (algae, bacteria, archaea) (2,3) that contribute to their ability to thrive at nearly all depths and latitudes. The endosymbionts, which can occupy >50 % of sponge volume (4), serve as energy source for sponges and provide a diverse pallet of metabolites and metabolic pathways that are beneficial to the sponge (reviewed in (2)). A prominent class of metabolites produced by the sponge and its endosymbionts are lipids. Lipid analysis of sponges started in the 1970s (5,6) and was sparked by the diversity and unique structures of fatty acids (FAs), of which extensive reviews exist (7–9). Characteristic of sponges is the presence of unusual poly-unsaturated, long chain (≥24 carbons(C)) FAs (LCFAs), with a typical $\Delta^{5,9}$ unsaturation (named “demospongic acids”, because of their first discovery in demosponges (5,10)). These LCFAs constitute a major part of sponge membrane phospholipids (PLs) and probably serve a structural and functional role (11). Sponges, because of their endosymbionts, are rich in bacterial FAs with high diversity, including not only the common *iso* (*i*) and *anteiso* (*a*)-branched FAs, but also more unusual ones. Typical of demosponges are a high abundance of mid-chain branched FAs (MBFAs), that are thought to be produced by sponge-specific eubacteria (12), and a presence of branched LCFAs (12,13). As branching is assumed to be introduced by microbes and not by the sponge host, the presence of branched LCFAs provides information on biosynthetic interactions between endosymbionts and host (12,14). Monoenic FA, e.g. $C_{16:1}\omega7$, abundant in bacteria (15), have been identified as precursors for LCFAs with ω7 configuration (16). Accordingly, the position of unsaturation also provides insight in bacteria-host biosynthetic interactions.

In addition, sponge FA composition may have taxonomic value, at least on a higher classification level (e.g. class level), since Demospongiae, Hexactinellida ('glass' sponges), Calcarea, and Homoscleromorpha have distinct FA profiles (17). However, the chemotaxonomic value on a lower classification level is disputable, since composition may alter with environmental conditions (18). The FA composition of sponges, especially combined with (natural abundance) stable isotope analysis, has been shown a valuable tool to infer dietary information on sponges, such as feeding on coral mucus (19), phytoplankton (20) and methane-fixing endosymbionts (21).

The North-Atlantic Ocean is home to extensive sponge grounds, that are widespread along the continental shelves, seamounts, and on the abyssal plains (22,23). *Geodiidae* and other sponge species of order Tetractinellida (class Demospongiae) are major constituents of these sponge grounds, representing >99 % of sponge ground benthic biomass (23–25). *Geodiidae* spp. are high microbial abundance (HMA) sponges that harbor rich, diverse and specific microbial communities (bacteria and archaea) involved in several biogeochemical processes, as observed in *G. barretti* (26). This is reflected in the FA composition of *G. barretti* that is dominated by bacterial FAs (12), including the distinct MBFAs that represent 28% of total FAs (12). However, the FA profiles of other *Geodiidae* are not described in the literature yet.

In this study we analyzed the FA profiles of five common deep-sea Tetractinellids, from different assemblages distinguished by temperature in the North Atlantic: the Arctic sponge ground assemblages accommodate *G. parva, G. hentscheli,* and *Stelletta* spp. (e.g. *S. rhaphidiophora*) dwelling at temperatures below 3–4 °C, and the boreal assemblages accommodate *G. barretti* and *G. atlantica* amongst others, which are typically found at temperatures above 3 °C (23,27). Based on the chemical configuration and the presence of branching in LCFAs, we propose biosynthetic pathways and show that these are consistent

with the C isotope ($\delta^{13}C$) signatures of LCFAs and bacterial precursors. The high abundance of endosymbiont markers that are precursors of LCFAs, indicate that these deep-sea sponges use their endosymbionts as metabolic source.

Methods

Sponge collection

Common habitat-building sponges of class Demospongiae, order Tetractinellida, were collected in the North-Atlantic Ocean by remotely operated vehicle (ROV) and box cores during different scientific expeditions. *G. atlantica (n* = 2) specimens were collected on the Sula Reef between 266–295 m depth during an expedition in August 2017 with the Norwegian research vessel G.O. Sars (64°42'N 7°59'E). *G. barretti* (*n* = 6) individuals were obtained from the Barents Sea (70°47N 18°03'E) around 300 m water depth on a subsequent G.O. Sars expedition in August 2018 (28). During the same expedition, *G. hentscheli, G. parva, Stelletta rhaphidiophora* (all *n* = 1) were collected at 550–600 m depth on the summit of Schulz Bank (73°50′ N, 7°34′ E) (29). *G. hentscheli* (*n* = 3)*, G. parva* (*n* = 3)*,* and *S. rhaphidiophora* (*n* = 2) specimens were retrieved on an Arctic expedition with the German research vessel Polarstern (AWI Expedition PS101) in September–October 2016 at 690–1000 m depth from Langseth Ridge, located in the permanently ice-covered Central Arctic (86°N,61°E). Sponges collected during the G.O. Sars expeditions were immediately dissected on board and sponges collected from Langseth Ridge were frozen at -20°C and dissected (frozen) in the lab. Subsamples (*n* = 3) from random parts of individual sponges were freeze-dried, grinded to obtain a fine powder. The powdered subsamples of sponges from Schulz Bank and Barents Sea were mixed to obtain a species representative sample, while a subsample of the interior of sponges was analyzed in case of Langseth Ridge specimens.

Lipid extraction and FAME preparation

Approximately 100 mg of sponge powder of each individual sponge was used per extraction. Sponge lipids were extracted with a modified Bligh and Dyer protocol (30), which was developed at NIOZ Yerseke (31–33). We adjusted this protocol by replacing chloroform with dichloromethane (DCM), because of lower toxicity. The whole protocol is available online: dx.doi.org/10.17504/protocols.io.bhnpj5dn. In short, sponge tissue samples were extracted in a solvent mixture (15 mL methanol, 7.5 mL DCM and 6 mL phosphate (P)-buffer (pH 7-8)) on a roller table for at least 3 hours. Layer separation was achieved by adding 7.5 mL DCM and 7.5 mL P-buffer. The DCM layer was collected, and the remaining solution was washed a second time with DCM. The combined DCM fraction was evaporated to obtain the total lipid extract (TLE), which was subsequently weighed. An aliquot of the TLE was separated into different polarity classes over an activated silica column. The TLE was first eluted with 7 mL DCM (neutral lipids), followed by 7 mL acetone (glycolipids) and 15 mL methanol (phospholipids). The phospholipid (PL) fraction, which was used for further analysis, was converted into fatty acid methyl esters (FAMEs) using alkaline methylation (using sodium methoxide in methanol with known $\delta^{13}C$). Alkaline methylation is recommended for complex lipid mixtures (34). After methylation, FAMEs were collected in hexane and concentrated to ~100 µL hexane for gas chromatography (GC) analysis.

For this study, two individual sponge samples per species were selected for detailed analysis. Aliquots of the FAME samples were used for double bond identification using dimethyl disulfide (DMDS) derivatization (35). Samples reacted overnight at 40°C in 50 µL hexane, 50 µL DMDS and 10 µL 60 mg/mL I_2. The reaction was stopped by adding 200 µL hexane and 200 µL $Na_2S_2O_3$. The hexane layer was collected, and the aqueous phase was washed twice with hexane. The combined hexane fraction was dried, subsequently eluted

over a small Na_2SO_4 column using in DCM: methanol (9:1) to remove any water and re-dissolved in hexane in a GC-vial for GC-analysis. Another aliquot of FAME sample was used for methyl-branching identification using catalytic hydrogenation with Adams catalyst (PtO_2) and hydrogen. Each FAME sample, dissolved in ~3 mL ethyl acetate with 10-30 mg PtO_2 and a drop of acetic acid, was bubbled with hydrogen gas for at least 1 h, after which the reaction vial was closed, and stirred overnight at room temperature. Subsequently, each sample was purified over a small column consisting of $MgSO_4$ (bottom) and Na_2CO_3 (top) using DCM and analyzed after re-dissolving it in ethyl acetate.

FAME analysis

FAMEs were analyzed on a gas chromatograph (GC) with flame ionization detector (FID) (HP 6890 series) for concentrations and GC-mass spectrometry (MS) (Finnigan Trace GC Ultra) for identification on a non-polar analytical column (Agilent, CP-Sil5 CB; 25 m x 0.32 mm x 0.12 µm). The GC oven was programmed from 70–130 °C at 20 °C/min and subsequently at 4 °C/min to 320 °C, at which it was hold for 20 min. The GC–FID was operated at a constant pressure of 100 kPa, whereas the GC–MS was operated at a constant flow of 2.0 mL min^{-1}. The MS was operated in Full Data Acquisition mode, scanning ions from *m/z* 50–800. The $^{13}C/^{12}C$ isotope ratios of individual FAMEs were determined by analyzing samples in duplicate on a GC-combustion-isotope ratio mass spectrometer (IRMS) consisting of a HP 6890N GC (Hewlett-Packard) connected to a Delta-Plus XP IRMS via a type-III combustion interface (Thermo Finnigan), using identical GC column and settings as for GC-MS.

Retention times were converted to equivalent chain length (ecl) based on the retention times of $C_{12:0}$, $C_{16:0}$, and $C_{19:0}$ FAMEs. The $\delta^{13}C$ values obtained by GC-C-IRMS were

corrected for the added C atom of the methylation agent. The data were analyzed and plotted in R (36) with R-package RLims (37).

Results

The lipid yield of *G. barretti, G. hentscheli, G parva,* and *S. rhaphidiophora* was similar, around 2–3 % of dry weight (DW). Only *G. atlantica* had a lower lipid yield, about 1.6 % of DW. The FA profiles of PL resembled those of TLE (Table S1). However, identification was more difficult using TLEs, because LCFAs co-eluted with sterols, hence PL chromatography was used for identification and composition analysis.

Identification

Chemical structures of individual FAs were identified by retention times (ecl), interpretation of their mass spectra and/or by identification using a NIST library. The assignments were verified with reference mixtures (bacterial and general FA mixtures from Sigma Aldrich) and by literature comparison (e.g. the reference ecl lists from NIOZ Yerseke (31)).

FAs are presented in both ω and Δ (IUPAC) annotation to avoid unambiguity and in a hybrid form, which is typical of sponge LCFA annotation (17,38) (Table 1). Unsaturation is described as $C_{x:y}$, where x is the number of C atoms and y is the number of double bonds, which is followed by Δ and all double bond positions from the carboxylic acid end in Δ notation, and the position of the first double bond from the methyl (terminal) end in ω notation (Table 1, Fig. 1). Methyl branching according to IUPAC notation is described as y-Me-C_x, where y is the position of the branching from the carboxylic acid end and x is the number of C atoms at the backbone, excluding the branching (Fig. 1). The ω notation follows

187 the terminology of IUPAC for MBFAs, but deviates for terminally branched FAs. The
188 penultimate (ω2) and pen-penultimate methyl branching (ω3) are described with ω notation
189 as *iso* (*i*-C_x) and *anteiso* (*a*-C_x) where x is the total number of C atoms, including the
190 branching (Table 1, Fig. 1).

191

192 **Table 1**: Fatty acid (FA) composition in % of total PLFA of deep-sea demosponge species
193 (order Tetractinellida): *Geodia atlantica* (*Ga*), *G. barretti* (*Gb*), *G. hentscheli* (*Gh*), *G. parva*
194 (*Gp*) and *Stelletta rhaphidiophora* (*Sr*). FA names are given in ω and Δ notation and a hybrid
195 form, with corresponding total C atoms (C) and equivalent chain length (ecl). FA categories
196 match with those of Fig. 2. Only FAs with abundance ≥1 % (in at least one species) are
197 shown. Numbers in bold are ≥ 10 % of total FAs.

			Species		*Ga*	*Gb*	*Gh*	*Gp*	*Sr*
FA notation			***n***		*2*	*6*	*4*	*4*	*3*
Ecl	**FA (ω)**	**FA (Δ)**	**C**	**Category**	**FA composition (%)**				
13.68	$C_{14:0}$	$C_{14:0}$	14	Other	0.9	1.0	1.0	0.8	1.5
14.17	Me-$C_{14:0}$	Me-$C_{14:0}$	15	Bacteria	0.7	1.4	1.4	1.3	1.8
14.38	*i*-$C_{15:0}$	13-Me-$C_{14:0}$	15		3.0	3.5	3.1	2.5	4.0
14.46	*a*-$C_{15:0}$	12-Me-$C_{14:0}$	15		2.6	2.6	2.2	2.0	4.3
15.35	Me-$C_{15:0}$	Me-$C_{15:0}$	16		0.6	0.9	1.6	1.8	1.6
15.59	$C_{16:1}\omega9$	$C_{16:1}\Delta^7$	16		1.6	0.5	2.6	3.3	2.5
15.68	$C_{16:1}\omega7$	$C_{16:1}\Delta^9$	16		6.3	8.7	7.8	6.3	8.2
15.78	$C_{16:1}\omega5$	$C_{16:1}\Delta^{11}$	16		1.5	2.1	1.9	1.6	2.7
16	$C_{16:0}$	$C_{16:0}$	16	Other	5.7	3.7	3.5	3.2	4.2
16.31	*i*-$C_{17:1}\omega7$	15-Me-$C_{16:1}\Delta^9$	17	Bacteria	4.2	5.4	1.4	1.0	1.4
16.45	8- and 9-Me-$C_{16:0}$	8- and 9-Me-$C_{16:0}$	17		8.3	**10**	**14**	**11**	**13**
16.62	*i*-$C_{17:0}$	15-Me-$C_{16:0}$	17		1.1	1.3	1.2	1.3	2.2
16.68	*a*-$C_{17:0}$	14-Me-$C_{16:0}$	17		1.4	1.3	0.9	0.8	1.2
17.40	Me-$C_{17:0}$	Me-$C_{17:0}$	18		3.1	2.8	1.7	1.9	2.0
17.65	$C_{18:1}\omega9$	$C_{18:1}\Delta^9$	18		1.2	0.2	1.5	1.4	1.5
17.72	$C_{18:1}\omega7$	$C_{18:1}\Delta^{11}$	18		3.1	4.2	3.8	3.9	3.7
18	$C_{18:0}$	$C_{18:0}$	18	Other	4.6	3.7	3.0	3.0	3.1
18.11	Me-$C_{18:1}\omega12$ or ω14	Me-$C_{18:1}\Delta^6$ or Δ^4	19	Bacteria	2.0	2.9	4.0	4.4	4.9
18.46	10- and 11-Me-$C_{18:0}$	10- and 11-Me-$C_{18:0}$	19		**12**	**17**	**20**	**23**	**19**
18.78	cy-$C_{19:0}$	cy-$C_{19:0}$	19		1.0	1.2	1.2	0.8	1.3
20.85	$C_{22:6}\omega3$	$C_{22:6}\ \Delta^{4,7,10,13,16,19}$	22	Other	1.8	1.3	0.2	0.6	
23.17	$C_{24:2}\Delta^{5,9}$ (ω15)	$C_{24:2}\Delta^{5,9}$	24	Sponge				1.2	
23.67	*i*-$C_{25:2}\Delta^{5,9}$ (ω15)	23-Me-$C_{24:2}\Delta^{5,9}$	25					**11**	

23.74	*a*-$C_{25:2}\Delta^{5,9}$ (ω15)	22-Me-$C_{24:2}\Delta^{5,9}$	25					4.2	
23.84	*i*-$C_{25:1}$ω7	23-Me-$C_{24:1}\Delta^{17}$	25		2.4	1.8			
24.73	$C_{26:2}\Delta^{5,9}$ (ω17)	$C_{26:2}\Delta^{5,9}$	26		2.4	2.4	5.4	0.4	0.4
24.81	$C_{26:2}\Delta^{9,19}$ (ω7)	$C_{26:2}\Delta^{9,19}$	26		4.3	8.4	8.5	0.6	
25.11	Me-$C_{26:2}\Delta^{5,9}$ (ω17)	Me-$C_{26:2}\Delta^{5,9}$	27		9.4	4.5	1.3		1.2
25.28	*(a)i*-$C_{27:2}\Delta^{5,9}$ (ω7) or $\Delta^{9,19}$ (ω17)	24 or 25-Me-$C_{26:2}\Delta^{5,9}$ or $\Delta^{9,19}$	27		4.9	2.9	0.1		0.7
25.96	$C_{28:2}\Delta^{5,9}$ (ω21)	$C_{28:2}\Delta^{5,9}$	28						1.5
26.14	$C_{28:2}\Delta^{11,21}$ (ω7)	$C_{28:2}\Delta^{11,21}$	28		1.9	1.8		3.6	
26.71	Me-$C_{28:2}\Delta^{5,9}$ (ω21)	Me-$C_{28:2}\Delta^{5,9}$	28						5.5

Fig. 1: Illustration of ω and Δ annotation for the chemical structure of *i*-$C_{17:1}$ω7 / 15-Me-$C_{16:1}\Delta^{9}$. The *a*(*i*) -notation for methyl branching describes the total number of C, while the Me-notation describes the number of C in the backbone. For sponge LCFAs, a mixture of both nomenclatures is, however, commonly used.

The elution order on an apolar column consists of FAMEs with methyl-branching close to the functional group to elute first, followed by the terminally (penultimate) branched *iso* (*i,* ω1) and pen-penultimate *anteiso* (*a,* ω2) FAMEs, and finally the unsaturated FAMEs, for which unsaturation closest to the functional group elutes first. Branched unsaturated FAMEs elute before branched straight FAMEs and straight FAMEs with the same C number elute last (Fig. 2, Table 1).

Figure 2: **GC trace of the FAME fraction extracted from demosponge *G. hentscheli* from Langseth Ridge (Central Arctic).** LCFA isomers often co-eluted or were at least not well separated as shown in this PLFA profile $C_{26:2}\Delta^{5,9}$ and $C_{26:2}\Delta^{9,19}$.

The position of branching was also verified with MS spectra, as *i*-branching was characterized by a more intense [M^+-43] fragment ion and *a*-branching was characterized by an elevated fragment ion at [M^+-57]. The position of methyl branching in saturated MBFAs

was identified via diagnostic mass fragments similar to (12). The relative intensity of *m/z* 171, 185, 199 and [185+213] was used to identify the relative contributions of 8, 9, 10, and 11-Me branching, respectively (Table S1). Because 11-Me-branching produces equal fragments of m/z 185 and 213, the excess of m/z 185 (213 – 185) was produced by 9-Me branching (Table S1) (12). The branching within unsaturated MBFAs was performed in hydrogenated samples, using similar diagnostic fragments and ecl of saturated FAMEs (Table S1).

Identification of unsaturation positions was conducted after treatment with DMDS, which is straight-forward with mono-unsaturated FAMEs. However, for poly-unsaturated FAMEs, identification with DMDS becomes complicated, because of multiple possibilities for S(-Me) adducts. The $\Delta^{5,9}$ unsaturation, typical of sponge LCFAs, forms a cyclic thioether at the C_6 and C_9 position along with methylthio groups at C_5 and C_{10} positions upon derivatization with DMDS. In addition, products are formed with either methylthio groups at C_5 and C_6 and a (unreacted) double bond at C_9 and C_{10}, and vice versa (39). This has been useful for identifying the typical $\Delta^{5,9}$ configuration in sponges (40).When unsaturation is far apart, i.e. positions $\Delta^{9,19}$ and $\Delta^{11,21}$, both double bonds are converted to dimethyl disulfide adducts (S1 Figure for their mass spectra). Based on ecl and a combination of DMDS and hydrogenation, we identified branched-monoenic and dienic FAs.

Fatty acid composition

The Arctic species (*G. hentscheli, G. parva, S. rhaphidiophora*) from Schulz Bank and Langseth Ridge had a similar FA profile (Table S1), so we pooled the compositional data from the two locations (Table 1). The data are standardized to % of total FAs to facilitate comparison, but actual concentrations (µg g^{-1} DW) are available in Table S1.

Bacterial fatty acids

Bacterial FAs, comprising branched and monoenic FAs with chain length < C_{20}, constituted the majority of total FAs in all five deep-sea demosponge species (67 ± 6 % mean ± SD of total FAs, used throughout text, n = 19, across all species) (Table 1, Fig. 3) and can represent up to 79 ± 2 % (in *S. rhaphidiophora*).

Fig. 3: **Average contribution of bacterial FAs (blue), sponge LCFAs (orange) and other FAs (green) to the total PLFAs of each species (abbreviated as in Table 1).**

MBFAs dominated the FA profiles of all deep-sea demosponge species (Table 1, Fig. 2), among them the most abundant were Me-$C_{18:0}$ (12–23 %, Table 1), with branching at 9, 10, 11 with a predominance at position 11 (*m/z* [213+185]; 49 % on average), followed by position 10 (*m/z* 199; 37 % on average). The second most abundant FAs were Me-$C_{16:0}$ (8–14 % of total FAs, Table 1), with branching at 8, 9, 10, 11 and a predominance of position 9 (*m/z* 185; 36 % on average) and 10 (*m/z* 199; 33 % on average). Also, Me-$C_{14:0}$, Me-$C_{15:0}$, and Me-$C_{17:0}$ were present, but in much lower abundance (≤ 3 % of total FAs for each, Table 1). Other branched (saturated) FAs found in all demosponges but less abundant, included *i*-$C_{15:0}$ (13-Me-$C_{14:0}$) and *a*-$C_{15:0}$ (12-Me-$C_{14:0}$) comprising 2–5 % of total FAs for each, and *i*-$C_{17:0}$ (15-Me-$C_{16:0}$) and *a*-$C_{17:0}$ (14-Me-$C_{16:0}$) ranging from 1 to 2 % of total FAs for each (Table 1).

Multiple monoenic FAs were found in the deep-sea demosponges. The most abundant were $C_{16:1}$ (ranging from 9 % in *G. atlantica* to 14 % in *G. parva* and *S. rhaphidiophora*), consisting of different isomers with the double bond at ω5, ω7, ω9, and ω11 positions. Isomers of $C_{18:1}$ with double bonds at ω7, ω8, ω9, ω11, ω12, ω13, ω14, and ω15 positions constituted 4–7 % of total FAs. The ω7 unsaturation dominated in both $C_{16:1}$ and $C_{18:1}$ FAs. In addition, rare $C_{16:1}$ and $C_{18:1}$ FAs with methyl-branching were found in demosponges. The

dominating unsaturation in $C_{16:1}$ was ω7 and the hydrogenated FAME sample indicated *i*-branching; *i*-$C_{17:1}$ω7 (15-Me-$_{16:1}\Delta^9$) represented 4–5 % in boreal species (*G. barretti, G. atlantica*) and < 2 % in Arctic species (*G. hentscheli, G. parva, S. rhaphidiophora*) (Fig. 1, Table 1). The most abundant unsaturation in $C_{18:1}$ FAs was ω12 (Δ^6) for *G. parva, G. hentscheli* and *S. rhaphidiophora* and ω14 (Δ^4) for *G. barretti* and *G. atlantica*, and the Me group was in the middle of the chain, since no increased peaks for *i*- and *a*-$C_{19:0}$ were found in the corresponding hydrogenated fractions. The mid-Me branched $C_{18:1}$ isomers (Me-$C_{18:1}$ω4 and Me-$C_{18:1}$ω12) were found in all demosponge species and ranged between 2–5 % (Table 1). Also, low amounts (< 1 %) of $C_{15:1}$ and non-branched $C_{17:1}$ were found.

Other fatty acids

Linear FAs were predominantly $C_{14:0}$, $C_{16:0}$ and $C_{18:0}$ in all species (Table1). Sponges contained only low amounts of FAs with a chain length between C_{20} and C_{24}, such as $C_{20:5}$ω3 (< 1 % in all species) and $C_{22:6}$ω3 (1.4 ± 0.9 %, n = 8) in boreal species *G. atlantica* and *G. barretti* and < 1% in Arctic species *G. hentscheli, G. parva* and *S. rhaphidiophora*.

Sponge fatty acids

LCFAs (≥ C_{24}), typical of sponges, differed per species and consisted of 24–29 C atoms (Table 1). LCFAs represented 21 ± 6 % (n = 19, across all species), with the highest contribution (29 %) in *G. atlantica* (Fig. 3). The most common unsaturation in demosponges was $\Delta^{5,9}$, but also unsaturation at $\Delta^{9,19}$ and $\Delta^{11,21}$ was observed.

- **C_{25}**: The dominant LCFA in *G. parva* was 23-Me-$C_{24:2}\Delta^{5,9}$ (*i*-$C_{25:2}\Delta^{5,9}$), followed by 22-Me-$C_{24:2}\Delta^{5,9}$ (*a*-$C_{25:2}\Delta^{5,9}$), making up 15 ± 1 % of total FAs. Isomers 23-Me-$C_{24:1}\Delta^{17}$ (*i*-$C_{25:1}$ω7) and (mid-)Me-$C_{24:1}\Delta^{17}$ (Me-$C_{24:1}$ω7) were present in boreal species (*G. atlantica* and *G. barretti*) representing together 2 ± 0.6 % (Table 1).

- **C_{26}**: The dominant LCFA in *G. hentscheli* was $C_{26:2}\Delta^{9,19}$, followed by $C_{26:2}\Delta^{5,9}$, together they represented 14 ± 6 % of total FAs in that species. *G. barretti* and *G. atlantica* also synthesized $C_{26:2}\Delta^{5,9}$ and $C_{26:2}\Delta^{9,19}$ in comparable amounts, representing together 11 ± 1% in *G. barretti* and 7 % in *G. atlantica.* Trace amounts (<1 %) of $C_{26:2}\Delta^{5,9}$ were present in *G. parva* and *S. rhaphidiophora.* Similarly, trace amount of $C_{26:2}\Delta^{11,21}$ (<1 %) was found in *G. parva*.
- **C_{27}**: (mid-)Me-$C_{26:2}\Delta^{5,9}$ were abundant in boreal species (*G. barretti*: 4 ± 3 %; *G. atlantica*: 9 %). Also 25-Me-$C_{26:2}\Delta^{5,9}$ (*i*-$C_{27:2}\Delta^{5,9}$), and 25-Me-$C_{26:2}\Delta^{9,19}$ (*i*-$C_{27:2}\Delta^{9,19}$) were produced by boreal species, representing together 3 ± 2 % of total FAs in *G. barretti* and 5 % in *G. atlantica.* Because these peaks co-eluted, the individual concentrations might represent isomeric mixtures. *G. hentscheli* possessed low amounts of (mid-)Me-$C_{26:2}\Delta^{5,9}$ and 25-Me-$C_{26:2}\Delta^{9,19}$ (*i*-$C_{27:2}\Delta^{9,19}$) (< 2 %). Similarly, *S. rhaphidiophora* had low amounts of (mid-)Me- $C_{26:2}\Delta^{5,9}$ and (*a*)*i*-$C_{27:2}\Delta^{5,9}$ (together 2 %, Table 1).
- **C_{28}**: *G. atlantica, G. barretti* and *G. parva* contained $C_{28:2}$ with $\Delta^{11,21}$ configuration, comprising 1.8 ± 1 % of total FAs in *G. barretti*, 1.9 % in *G. atlantica* and 3.6 ± 1.7 % in *G. parva*. *S. rhaphidiophora* contained a low amount of $C_{28:2}\Delta^{5,9}$ (1.5 ± 0.4 %) (Table 1).
- **C_{29}:** The dominant LCFA in *S. rhaphidiophora* was (mid)-Me-$C_{28:2}\Delta^{5,9}$ with a contribution of 5.5 ± 0.6 % to total FAs (Table 1).

Stable C isotope values ($\delta^{13}C$)

Stable C isotope values ($\delta^{13}C$) of dominant FAs ranged between -18 ‰ (95 percentile) and -26 ‰ (5 percentile) and showed similar patterns across all demosponges (Fig. 4, Table 2). The $\delta^{13}C$ values of the dominant MBFAs, Me-$C_{16:0}$, Me-$C_{18:0}$, and also Me-$C_{18:1}\omega12$ (and

ω14) were enriched in ^{13}C compared to other bacterial fatty acids, (*a(i)*-$C_{15:0}$, $C_{16:1}\omega7$, $C_{18:1}\omega7$) (Fig. 4, Table 2). The most depleted FA was *i*-$C_{17:1}\omega7$ (-25.7 ± 1.3 ‰ $\delta^{13}C$). The different LCFA isomers were analyzed as one, because isomers co-eluted or were at least not well separated on GC (Fig. 2). However, we could assign separate isotope values for (*a)i*-$C_{27:2}$ and Me-$C_{26:2}$ (Fig. 4). The LCFAs showed less isotopic variation compared to bacterial FAs, but still ranged between -25 and -19 ‰ (5–95 percentile) (Fig. 4, Table 2). Me-$C_{26:2}$ and (*a*)*i*-$C_{27:2}$ had relatively similar $\delta^{13}C$ values, -20 and -21 ‰, in *G. barretti* and *G. atlantica,* but a more prominent difference of -21 and -24 ‰ was observed in the hydrogenated samples (n = 1 per species), indicating that peak overlap blurred the isotopic values.

Table 2: $\delta^{13}C$ values (mean ± SD) of (bacterial) FA precursors and dominant LCFAs of all species combined.

Category	Fatty acid biomarker	Average $\delta^{13}C$ (‰) ± SD
a(i)-branched FA	(*a*)*i*-$C_{15:0}$	-22.8 ± 0.6
	(*a*)*i*-$C_{25:2}$	-22.0 ± 0.6
	i-$C_{17:1}\omega7$	-25.7 ± 1.3
	i- $C_{25:1}\omega7$	-23.9 ± 0.7
	(*a*)*i*-$C_{27:2}$	-21.0 ± 1.2
Linear FA	$C_{16:0}$	-21.6 ± 1.1
	$C_{18:0}$	-20.2 ± 1.2
	$C_{16:1}\omega7$	-23.0 ± 2.0
	$C_{18:1}\omega7$	-23.6 ± 1.5
	$C_{26:2}$	-21.8 ± 0.9
	$C_{28:2}$	-23.2 ± 1.4
Mid-branched FA	Me-$C_{16:0}$	-19.3 ± 1.6
	Me-$C_{18:0}$	-18.4 ± 1.1
	Me-$C_{18:1}$	-17.4 ± 1.3
	Me-$C_{26:2}$	-20.2 ± 0.6
	Me-$C_{28:2}$	-19.4 ± 0.2

Fig. 4: $\delta^{13}C$ composition of precursors and dominant LCFAs in analyzed demosponges. Sponge species were pooled together, and the median is indicated in the box plot as black

line. The numbers depict the sample size (individual FAME samples). The colors are used to match bacterial precursor FAs with sponge-produced LCFAs. Pink is used for (mid-)Me-branched FAs, grey is used for linear FAs, blue and yellow indicate *(a)i*-branched FAs with distinct $\delta^{13}C$ that may end up in an isomeric mixture, indicated by green (see Fig. 5 for biosynthetic pathways).

Discussion

Bacterial FAs

High concentrations of isomeric mixtures of MBFAs were found in all five sponge species analyzed, independent of species and location (Table 1). A predominance of MBFAs is considered to be a typical feature of Demospongiae, because it is not observed in any other organism, sediment or water (12,17,41). Typical position of branching is between ω5 and ω9 (12), resulting in predominance of 8- and 9-Me-$C_{16:0}$ and 10- and 11-Me-$C_{18:0}$ in this study, in agreement with previously reported MBFAs (42,43). MBFAs are typically produced by bacteria, so they are presumably made by distinctive and sponge-specific eubacterial symbionts. It has been hypothesized that these bacteria were widespread in the geological past and were inherited in the protective environment of distinctive sponge hosts in modern marine environments (8,12). This hypothesis has been further supported by genomic analysis on *Geodia* sp. revealing similar microbial communities between species with little geographical variation (44).

A proposed candidate phylum for MBFAs is Poribacteria, a unique and abundant phylum in HMA sponges (45), since a positive relation between MBFA concentration and Poribacteria abundance was found across several sponge species (43). Metagenome analyses showed that Poribacteria are a prominent phylum in *G. barretti* (46,47), but are rare or even

359 absent in *G. hentscheli* (48), which shows a dominance of Acidobacteria, Chloroflexi, and
360 Proteobacteria, phyla that are also abundant in *G. barretti* (46,47). This suggests that either
361 the MBFAs belong to one of the above-mentioned phyla, or that the MBFAs are shared
362 among microbial phyla, as their chemotaxonomic resolution is lower compared to genomic
363 analysis. In the environment, MBFAs are primarily found in nitrogen and sulfur reducers
364 (chemoheterotrophs) and oxidizers (chemoautotrophs) that are mostly members of the (large)
365 proteobacteria family (49–52). Nitrogen and sulfur reduction and oxidation processes are
366 conducted in deep-sea sponges such as *G. barretti* (26,53,54), and oxidation processes are
367 coupled to CO_2 fixation, although associated CO_2 fixation is likely to contribute < 10 % of
368 the carbon demand of deep-sea sponges (55). The poribacteria in sponges were also
369 characterized as mixotrophic bacteria, able to fix CO_2 using the ancient Wood–Ljungdahl
370 (reversed acetyl-CoA) pathway (56). The isotopic enrichment in MBFAs (Fig. 4, Table 2),
371 agrees with earlier observations for *G. barretti* (57), and might thus be linked to nitrogen and
372 sulfur transforming processes and potentially CO_2 fixation. It will be interesting to perform
373 an isotope-tracer study (55) with ^{13}C-CO_2 to assess CO_2 incorporation in the abundant
374 MBFAs, perhaps combined with nitrification (or sulfur oxidation) inhibitors, similar to
375 Veuger et al. (58).

376 The most depleted FA (*i*-$C_{17:1}\omega7$, Fig. 4, Table 2) is considered a chemotaxonomic
377 marker for the sulfur reducing bacteria *Desulfovibrio* sp. (59). The isotopic difference
378 between *i*-$C_{17:1}\omega7$ and MBFAs suggest that these markers are not from the same microbial
379 consortium. The more general bacterial markers (e.g. *(a)i*-$C_{15:0}$, typical of gram-positive
380 bacteria and $C_{16:1}\omega7$ and $C_{18:1}\omega7$, typical of general gram-negative bacteria (15)) had
381 intermediate $\delta^{13}C$ values (Fig. 4, Table 2). Such values can be the result of isotopic averages
382 from different pathways, since they are more general bacterial markers, or they might

represent general heterotrophy on organic matter with $\delta^{13}C$ value from -24 to -22 ‰ in the western Arctic (60).

The low contribution of FAs with a chain length of C_{20} to C_{24} typical of phytoplankton and zooplankton (e.g. $C_{20:5}\omega3$ and $C_{22:6}\omega3$) indicates that sinking zoo- and phytoplankton are not contributing much to sponge diet, at least not directly. These findings support increasing evidence that *G. barretti* (and other North-Atlantic deep-sea sponges) primarily feed on dissolved organic matter and pelagic and associated bacteria (61,62). A higher contribution of phytoplankton markers in boreal *Geodia* spp. (*G. atlantica* and *G. barretti*) compared to Arctic species (Table 1) might be linked to water depth, as boreal species were sampled from ~300 m and Arctic species from ~600 m, while also environmental factors, such as permanent ice coverage (Langseth Ridge) and a generally lower primary production in the Arctic compared to the boreal North-Atlantic ocean (63) might play a major role.

The overall high abundance of bacterial FAs (56–79 % of total FAs across all five analyzed deep-sea demosponge species, Fig. 3) fits with their classification as HMA sponges and supports the idea that microbial endosymbionts play a pivotal role in sponge metabolism (2,3). It is important to notice that the contribution of endosymbionts is likely even higher, since archaea are not detected with (PL)FA analysis (64), while they were also found to be abundant in *G. barretti* (46,47).

Sponge LCFAs

Although bacterial FA profiles were very similar among the studied Tetractinellid species, the sponge-specific LCFA composition was more species-specific. The dominant unsaturation in LCFAs, was double unsaturation at $\Delta^{5,9}$ position in all species analyzed, which is typical feature of demosponges (5,10). Similarly, the linear $C_{26:2}\Delta^{5,9}$, (*a*)*i*-$C_{25:2}\Delta^{5,9}$

and/or *i*-$C_{27:2}\Delta^{5,9}$, present in all species analyzed (Fig. 5, Table 1), are common LCFAs of demosponges, (e.g. (17,38,65), for an overview see (8)). We found (mid-)Me-branched $\Delta^{5,9}$ LCFAs in all species, except *G. parva* (Fig. 5, Table 1). Also, Thiel et al. (17) found them in *G. barretti* and some other Demospongiae (*Haliclona* sp.*, Petrosia* sp.) but not in all analyzed Demospongiae. We also identified novel LCFAs: *i*-$C_{27:2}\Delta^{9,19}$ (in *G. atlantica, G. barretti,* and *G. hentscheli*) and $\Delta^{11,21}$ in $C_{26:2}$ and $C_{28:2}$ (*G. barretti* and *G. parva*). The presence of Δ^{11} unsaturation ($C_{26:2}\Delta^{11,21}$ and $C_{28:2}\Delta^{11,21}$), identified via DMDS derivatization, is uncommon in sponge LCFAs. Barnathan et al. (66) found Δ^{11} unsaturation in a series of monoenic FAs, including $C_{28:1}$, in a tropical demosponge species (order Axinellida), but no dienic LCFAs with Δ^{11} unsaturation have been described so far. The configuration indicates that Δ^{11} desaturase might be active in these species; however, the activity of this enzyme in sponges has not been reported.

G. atlantica and *G. barretti* had almost identical FA profiles (Table 1), suggesting that these species might be closely related, as was earlier suggested based on their sterol and amino acid composition (67), but deviates from molecular phylogeny that places them further apart (27). The FA profile of *G. hentscheli* resembled those of *G. barretti* and *G. atlantica* and based on molecular phenology, *G. hentscheli* is a sister species of *G. barretti*. On the other hand, *G. parva* produced distinct LCFAs compared to the other *Geodia* spp., the *i*- and *a*-$C_{25:2}\Delta^{5,9}$ and this species is also phylogenetically apart from the other *Geodia* spp. (27). A dominance of *(a)i*-branched $C_{25:2}$ has been found in another Geodiidae family (*Geodinella)* (68). Finally, also *S. rhaphidiophora* produced a distinct LCFA, Me-$C_{28:2}\Delta^{5,9}$, a LCFA that has been described for demosponges of the family *Aplysinidae* (13,42).

Each of the three dominant Tetractinellids of Artic sponge grounds (*G. hentscheli, G. parva* and *S. rhaphidiophora)* produced distinct LCFAs (Table 1) that can serve as chemotaxonomic markers. The morphology of these sponges is very similar, so LCFA

433 analysis provides an additional method to identify each species. Furthermore, the distinct
434 LCFAs could be useful as trophic markers to study the ecological role of deep-sea sponges in
435 the environment. No geographical differences in LCFA composition of Arctic Tetractinellids
436 were found (Table S1) suggesting that the environment has a limited influence on the LCFA
437 composition, which is a prerequisite for using LCFA as chemotaxonomic markers.
438

439 **Biosynthetic pathways of prominent sponge fatty acids**

440 The identification of branching in LCFAs allows identification of its short chain
441 precursors and biosynthetic pathways. As demonstrated by various *in vivo* incorporation
442 studies with radioactive substrates (16,38,65,69), sponges elongate FA precursors by adding
443 2 C atoms at the carboxylic acid end and desaturate at Δ^5 and Δ^9 (visualized in (10)),
444 revealing $C_{16:0}$ as precursor for the common $C_{26:2}\Delta^{5,9}$, while $C_{16:1}\omega7$ was identified as
445 precursors for $C_{26:2}\Delta^{9,19}$ (Fig. 5). There is no evidence for branching to be introduced by
446 sponges, so *i*- and *a*-$C_{15:0}$ were identified as precursors of *i*- and *a*-$C_{27:2}\Delta^{5,9}$ (Fig. 5) (38),
447 while Me-$C_{16:0}$ has been identified as precursor for Me-$C_{26:2}\Delta^{5,9}$ and Me-$C_{28:2}\Delta^{5,9}$ (Fig. 5)
448 (13,16,70). Finally, we hypothesize that *i*-$C_{17:1}\omega7$ is the precursor for *i*-$C_{25:1}\omega7$ and *i*-
449 $C_{27:2}\Delta^{9,19}$ found in *G. atlantica, G. barretti,* and *G. hentscheli* (Fig. 5).

450 Application to the present study showed that most LCFAs could be linked to
451 precursors via established pathways, with hypothetical intermediates since hardly any were
452 found in detectable abundance (Fig. 5). The C isotopic differences in bacterial precursors
453 were (partially) reflected in C isotopic composition of LCFAs (Fig. 4, Table 2), although the
454 differences were not as prominent in LCFAs compared to their precursors. One explanation is
455 that a mixture of C sources is used by the host to elongate precursors to LCFAs, while also
456 methodological aspects might contribute. A (much) longer analytical column might help
457 improving separation of LCFAs.

458

459 **Fig. 5**: **Proposed biosynthetic pathways of (microbial) precursors to LCFA in examined**
460 **Tetractinellid species.** FAs detected in the studied sponges are shown in a black rectangle,
461 solid arrows indicate elongation, dashed arrows indicate $\Delta^{5,9}$ desaturation. The species
462 encompassing each LCFA are indicated with abbreviated names as in Table 1 and names in
463 bold means that the LCFA is dominant in that specific species.

464

465 The schematization of Fig. 5 shows the benefit of using both ω and Δ (and mixed)
466 nomenclatures in sponge lipid research. Annotations from the terminal end (ω and *(a)i*
467 notation) (Fig. 1) are convenient to show biosynthetic pathways as these positions do not
468 change with elongation (Fig. 5). However, the typical $\Delta^{5,9}$ unsaturation is more convenient to
469 show with Δ annotation, as an ω notation would alter with varying C chain length (Fig. 5).
470 Ambiguity arises in ω notation of methyl-branching, because *a(i)* notation is used for
471 terminally branched FAs and describes total C atoms (including the methyl group(s)), while
472 Me notation is used for MBFAs and describes the C number of the backbone (excluding
473 methyl group (s)) and counts the position of the branching from the carboxylic acid end (and
474 not the terminal (ω) end, Fig. 1). This might lead to confusion about the total C number,
475 which is needed to correct measured isotope values for the extra methyl group, and about the
476 ω position of unsaturation (start counting from the end of the backbone, excluding the
477 methyl-group) and the conversion from ω to Δ notation (Fig. 1). We added this discussion to
478 create awareness and would like to recommend including a description of the notation in the
479 methods and presenting both nomenclature when a mixture of notation styles is used.

480

Conclusions

In this study we identified FAs of prominent habitat-building demosponges (order Tetractinellida) from the boreal-Arctic Atlantic Ocean. All five species investigated contained predominantly bacterial FAs, in particular isomeric mixtures of MBFAs (Me-$C_{16:0}$ and Me-$C_{18:0}$) (together >20% of total FAs). The MBFAs were isotopically enriched compared to linear and (*ante*)*iso*-branched FAs. The sponge-produced LCFAs with chain lengths of C_{24}-C_{28} were linear, mid- and *a(i)*-branched and had predominantly the typical $\Delta^{5,9}$ saturation. They also produced (yet undescribed) branched and linear LCFAs with $\Delta^{9,19}$ and $\Delta^{11,21}$ unsaturation, namely *i*-$C_{27:2}\Delta^{9,19}$, $C_{26:2}\Delta^{11,21}$, and $C_{28:2}\Delta^{11,21}$. *G. parva* and *S. rhaphidiophora* each produced distinct LCFAs, while *G. atlantica, G. barretti,* and *G. hentscheli* had a similar LCFA profile, although each species had different predominant ones. The typical FA profiles of North-Atlantic deep-sea demosponges can be used as chemotaxonomic and trophic markers. We proposed biosynthetic pathways for dominant LCFAs from their bacterial precursors, which were supported by small isotopic differences in LCFAs that support the idea that sponges acquire building blocks from their endosymbiotic bacteria.

Acknowledgements

We thank Antje Boetius for supporting and promoting this study and organizing the PS101. We thank the captain and crew of PS101 for excellent support at sea. We thank late Hans Tore Rapp (UiB) for organizing the G.O. Sars expeditions and excellent project coordination. We thank Desmond Eefting for analytical assistance. We thank master students Gydo Geijer, Sean Hoetjes, David Lenkes, Floor Wille, and Femke van Dam for their help in the lab and with analyses. We thank Eva de Rijke, Samira Absalah and Stefan Schouten for

their help in protocol development. Irene Rijpstra and Volker Thiel are acknowledged for their help with FA identification. We thank Pieter van Rijswijk and Marco Houtekamer for sharing their analytical knowledge and identification libraries. Paco Cardenas is acknowledged for sharing his taxonomic knowledge.

References

1. van Soest RWM, Boury-Esnault N, Vacelet J, Dohrmann M, Erpenbeck D, de Voogd NJ, et al. Global diversity of sponges (Porifera). PLoS One. 2012;7(4).
2. Taylor MW, Radax R, Steger D, Wagner M. Sponge-Associated microorganisms: evolution, ecology, and biotechnological potential. Microbiol Mol Biol Rev. 2007;71(2):295–347.
3. Pita L, Rix L, Slaby BM, Franke A, Hentschel U. The sponge holobiont in a changing ocean: from microbes to ecosystems. Microbiome. 2018;6(1):46.
4. Ribes M, Jiménez E, Yahel G, López-Sendino P, Diez B, Massana R, et al. Functional convergence of microbes associated with temperate marine sponges. Environ Microbiol. 2012;14(5):1224–39.
5. Litchfield C, Greenberg AJ, Noto G, Morales RW. Unusually high levels of C24-C30 fatty acids in sponges of the class demospongiae. Lipids. 1976;11(7):567–70.
6. Morales RW, Litchfield C. Unusual C24, C25, C26 and C27 polyunsaturated fatty acids of the marine sponge *Microciona prolifera*. Biochim Biophys Acta, Lipids Lipid Metab. 1976;431:206–16.
7. Rod'kina SA. Fatty acids and other lipids of marine sponges. Russ J Mar Biol. 2005;31:S49–60.
8. Rezanka T, Sigler K. Odd-numbered very-long-chain fatty acids from the microbial , animal and plant kingdoms. Prog Lipid Res J. 2009;48(3-4):206–38.

9. Mishra PM, Sree A, Panda P. Fatty acids of Marine sponges. In: Kim SK (eds), Springer handbook of marine biotechnology. Springer Berlin Heidelberg; 2015. p. 851–68.

10. Kornprobst JM, Barnathan G. Demospongic acids revisited. Mar Drugs. 2010;8(10):2569–77.

11. Lawson MP, Thompson JE, Djerassi C. Cell membrane localization of long chain C24-C30 fatty acids in two marine demosponges. Lipids. 1988;23(8):741–9.

12. Thiel V, Jenisch A, Wörheide G, Löwenberg A, Reitner J, Michaelis W. Mid-chain branched alkanoic acids from "living fossil" demosponges: A link to ancient sedimentary lipids? Org Geochem. 1999;30(1):1–14.

13. Raederstorff D, Shu AYL, Thompson JE, Djerassi C. Biosynthetic studies of marine lipids. 11.1 Synthesis, biosynthesis, and absolute configuration of the internally branched demospongic acid, 22-Methyl-5,9-octacosadienoic acid. J Org Chem. 1987;52(12):2337–46.

14. Bergé J-P, Barnathan G. Fatty acids from lipids of marine organisms: molecular biodiversity, roles as biomarkers, biologically active compounds, and economical aspects. Mar Biotechnol. 2005;1:51–111.

15. Zelles L. Phospholipid fatty acid profiles in selected members of soil microbial communities. Chemosphere. 1997;35(1–2):275–94.

16. Djerassi C, Lam WK. Sponge Phospholipids. Acc Chem Res. 1991;24(3):69–75.

17. Thiel V, Blumenberg M, Hefter J, Pape T, Pomponi S, Reed J, et al. A chemical view of the most ancient metazoa - Biomarker chemotaxonomy of hexactinellid sponges. Naturwissenschaften. 2002;89(2):60–6.

18. Lawson MP, Bergquist PR, Cambie RC, Lawson MP, Lavis A, Cambie RC. Fatty acid composition and the classification of the Porifera. Biochem Syst Ecol. 1984;12(1):63–

555 84.

556 19. van Duyl FC, Moodley L, Nieuwland G, van IJzerloo L, van Soest RWM, Houtekamer
557 M, et al. Coral cavity sponges depend on reef-derived food resources: Stable isotope
558 and fatty acid constraints. Mar Biol. 2011;158(7):1653–66.

559 20. Thurber AR. Diets of Antarctic sponges: Links between the pelagic microbial loop and
560 benthic metazoan food web. Mar Ecol Prog Ser. 2007;351:77–89.

561 21. Rubin-Blum M, Antony CP, Sayavedra L, Martínez-Pérez C, Birgel D, Peckmann J, et
562 al. Fueled by methane: Deep-sea sponges from asphalt seeps gain their nutrition from
563 methane-oxidizing symbionts. ISME. 2019;13:1209–1225.

564 22. Knudby A, Kenchington E, Murillo FJ. Modeling the distribution of *Geodia* sponges
565 and sponge grounds in the Northwest Atlantic. PLoS One. 2013;8(12):1–20.

566 23. Klitgaard AB, Tendal OS. Distribution and species composition of mass occurrences
567 of large-sized sponges in the northeast Atlantic. Prog Oceanogr. 2004;61(1):57–98.

568 24. Kutti T, Bannister RJ, Fosså JH. Community structure and ecological function of deep-
569 water sponge grounds in the Traenadypet MPA-Northern Norwegian continental shelf.
570 Cont Shelf Res. 2013;69:21–30.

571 25. Murillo FJ, Muñoz PD, Cristobo J, Ríos P, González C, Kenchington E, et al. Deep-
572 sea sponge grounds of the Flemish Cap, Flemish Pass and the Grand Banks of
573 Newfoundland (Northwest Atlantic Ocean): Distribution and species composition. Mar
574 Biol Res. 2012;8(9):842–54.

575 26. Hoffmann F, Larsen O, Thiel V, Rapp HT, Pape T, Michaelis W, et al. An anaerobic
576 world in sponges. Geomicrobiol J. 2005;22:1–10.

577 27. Cardenas P, Rapp HT, Klitgaard AB, Best M, Thollesson M, Secher Tendal O.
578 Taxonomy, biogeography and DNA barcodes of *Geodia* species (Porifera,
579 Demospongiae, Tetractinellida) in the Atlantic boreo-arctic region. Zool J Linn Soc.

2013;169(2):312–61.

28. Bart MC, Kluijver A De, Hoetjes S, Absalah S, Mueller B, Rapp HT, et al. Differential processing of dissolved and particulate organic matter by deep-sea sponges and their microbial symbionts. Sci Rep. Forthcoming.

29. Roberts EM, Mienis F, Rapp HT, Hanz U, Meyer HK, Davies AJ. Oceanographic setting and short-timescale environmental variability at an Arctic seamount sponge ground. Deep Res Part I Oceanogr Res Pap. 2018;138:98–113.

30. Bligh EG, Dyer WJ. A rapid method of total lipid extraction and purification. Can J Biochem Physiol. 1959;37(8):911–17.

31. Koopmans M, Rijswijk P Van, Martens D, Wijffels RH. Seasonal variation of fatty acids and stable carbon isotopes in sponges as indicators for nutrition : biomarkers in sponges identified. Mar biotechnol. 2015;17(1):43–54.

32. Rix L, de Goeij JM, Mueller CE, Struck U, Middelburg JJ, van Duyl FC, et al. Coral mucus fuels the sponge loop in warm- and cold-water coral reef ecosystems. Sci Rep. 2016;6:18715.

33. Boschker HTS. Linking microbial community structure and functioning: stable isotope (^{13}C) labeling in combination with PLFA analysis. In: Kowalchuk GA, de Bruijn FJ et al. (eds), Molecular microbial ecology manual. 2nd edition. Kluwer-Academic publishers; 2004. p. 1673–88.

34. Christie WW. Preparation of Ester Derivatives of Fatty Acids for Chromatographic Analysis. Adv Lipid Methodol. 1993;69–111.

35. Nichols PD, Guckert JB, White DC. Determination of monosaturated fatty acid double-bond position and geometry for microbial monocultures and complex consortia by capillary GC-MS of their dimethyl disulphide adducts. J Microbiol Methods. 1986;5(1):49–55.

605 36. Team RC. R: A language and environment for statistical computing. R Foundation for
606 Statistical Computing. 2019.
607 37. Soetaert K, Provoost P, Van Rijswijk P. RLims: R functions for Lab Analysis using
608 GC-FID and GC-c-IRMS. 2015.
609 38. Carballeira N, Thompson JE, Ayanoglu E, Djerassi C. Biosynthetic Studies of Marine
610 Lipids. 5. The biosynthesis of long-chain branched fatty acids in marine sponges. J Org
611 Chem. 1986;51(14):2751–6.
612 39. Vincenti M, Guglielmetti G, Cassani G, Tonini C. Determination of double bond
613 position in diunsaturated compounds by mass spectrometry of dimethyl disulfide
614 derivatives. Anal Chem. 1987;59(5):694–9.
615 40. Carballeira NM, Shalabi F. Unusual lipids in the Caribbean sponges *Amphimedon*
616 *viridis* and *Desmapsamma anchorata*. J Nat Prod. 1994;57(8):1152–9.
617 41. Gillan FT, Stoilov IL, Thompson JE, Hogg RW, Wilkinson CR, Djerassi C. Fatty acids
618 as biological markers for bacterial symbionts in sponges. Lipids. 1988;23(12):1139–
619 45.
620 42. Nechev J, Christie WW, Robaina R, De Diego F, Popov S, Stefanov K. Lipid
621 composition of the sponge *Verongia aerophoba* from the Canary islands. Eur J Lipid
622 Sci Technol. 2002;104(12):800–7.
623 43. Hochmuth T, Niederkrüger H, Gernert C, Siegl A, Taudien S, Platzer M, et al. Linking
624 chemical and microbial diversity in marine sponges: Possible role for poribacteria as
625 producers of methyl-branched fatty acids. ChemBioChem. 2010;11(18):2572–8.
626 44. Schöttner S, Hoffmann F, Cárdenas P, Rapp HT, Boetius A, Ramette A. Relationships
627 between host phylogeny, host type and bacterial community diversity in cold-water
628 coral reef sponges. PLoS One. 2013;8(2):1–11.
629 45. Fieseler L, Horn M, Wagner M, Hentschel U. Discovery of the novel candidate

630 phylum “Poribacteria” in marine sponges. Appl Environ Microbiol. 2004;70(6):3724–
631 32.
632 46. Radax R, Rattei T, Lanzen A, Bayer C, Rapp HT, Urich T, et al. Metatranscriptomics
633 of the marine sponge *Geodia barretti* : tackling phylogeny and function of its
634 microbial community. 2012;14:1308–24.
635 47. Luter HM, Bannister RJ, Whalan S, Kutti T, Pineda MC, Webster NS. Microbiome
636 analysis of a disease affecting the deep-sea sponge *Geodia barretti*. FEMS Microbiol
637 Ecol. 2017;93(6):1–6.
638 48. Busch K, Hanz U, Mienis F, Mueller B, Franke A, Martyn Roberts E, et al. On giant
639 shoulders: How a seamount affects the microbial community composition of seawater
640 and sponges. Biogeosciences. 2020;17(13):3471–86.
641 49. Kool DM, Zhu B, Rijpstra WIC, Jetten MSM, Ettwig KF, Sinninghe Damsté JS. Rare
642 branched fatty acids characterize the lipid composition of the intra-aerobic methane
643 oxidizer “*Candidatus* Methylomirabilis oxyfera.” Appl Environ Microbiol.
644 2012;78(24):8650–6.
645 50. Kerger B, Nichols PD, Antworth CP, Sand W, Bock E, Cox JC, et al. Signature fatty
646 acids in the polar lipids of acid-producing Thiobacillus spp .: methoxy , cyclopropyl ,
647 alpha-hydroxy-cyclopropyl and branched and normal monoenoic fatty acids. FEMS
648 Microbiol Ecol. 1986;2(2):67–77.
649 51. Schwab VF, Herrmann M, Roth VN, Gleixner G, Lehmann R, Pohnert G, et al.
650 Functional diversity of microbial communities in pristine aquifers inferred by PLFA-
651 and sequencing-based approaches. Biogeosciences. 2017;14(10):2697–714.
652 52. Lipski A, Spieck E, Makolla A, Altendorf K. Fatty acid profiles of nitrite-oxidizing
653 bacteria reflect their phylogenetic heterogeneity. Syst Appl Microbiol.
654 2001;24(3):377–84.

655 53. Hoffmann F, Radax R, Woebken D, Holtappels M, Lavik G, Rapp HT, et al. Complex
656 nitrogen cycling in the sponge *Geodia barretti*. Environ Microbiol. 2009;11(9):2228–
657 43.
658 54. Radax R, Hoffmann F, Rapp HT, Leininger S, Schleper C. Ammonia-oxidizing
659 archaea as main drivers of nitrification in cold-water sponges. Environ Microbiol.
660 2012;14(4):909–23.
661 55. van Duyl FC, Lengger SK, Schouten S, Lundälv T, van Oevelen D, Müller CE. Dark
662 CO_2 fixation into phospholipid-derived fatty acids by the cold-water coral associated
663 sponge *Hymedesmia (Stylopus) coriacea* (Tisler Reef, NE Skagerrak). Mar Biol Res.
664 2020;16(1):1–17.
665 56. Siegl A, Kamke J, Hochmuth T, Piel J, Richter M, Liang C, et al. Single-cell genomics
666 reveals the lifestyle of Poribacteria, a candidate phylum symbiotically associated with
667 marine sponges. ISME J. 2011;5(1):61–70.
668 57. Pape T. Lipidbiomarker Schwammassoziierter Bakterien Und Archaeen. Doctoral
669 dissertation. University of Hamburg. 2004 Available from: https://ediss.sub.uni-
670 hamburg.de/volltexte/2004/2112/
671 58. Veuger B, Pitcher A, Schouten S, Sinninghe Damsté JS, Middelburg JJ. Nitrification
672 and growth of autotrophic nitrifying bacteria and Thaumarchaeota in the coastal North
673 Sea. Biogeosciences. 2013;10(3):1775–85.
674 59. Boon JJ, De Leeuw JW, Van De Hoek GJ, Vosjan JH. Significance and taxonomic
675 value of iso and anteiso monoenoic fatty acids and branched β hydroxy acids in
676 *Desulfovibrio desulfuricans*. J Bacteriol. 1977;129(3):1183–91.
677 60. Griffith DR, McNichol AP, Xu L, McLaughlin FA, MacDonald RW, Brown KA, et al.
678 Carbon dynamics in the western Arctic Ocean: Insights from full-depth carbon isotope
679 profiles of DIC, DOC, and POC. Biogeosciences. 2012;9(3):1217–24.

680 61. Leys SP, Kahn AS, Fang JKH, Kutti T, Bannister RJ. Phagocytosis of microbial
681 symbionts balances the carbon and nitrogen budget for the deep-water boreal sponge
682 *Geodia barretti*. Limnol Oceanogr. 2018;1–16.
683 62. Bart M, Mueller B, Rombouts T, van de Ven C, Tompkins G, Osinga R, et al.
684 Dissolved organic carbon (DOC) is essential to balance the metabolic demands of
685 North-Atlantic deep-sea sponges. BioRxiv [Preprint].2020 bioRxiv 305086 [posted
686 2020 Sep 21]. Available from:
687 https://www.biorxiv.org/content/10.1101/2020.09.21.305086v1
688 63. Wassmann P, Slagstad D, Ellingsen I. Primary production and climatic variability in
689 the European sector of the Arctic Ocean prior to 2007: Preliminary results. Polar Biol.
690 2010;33(12):1641–50.
691 64. Koga Y, Morii H. Biosynthesis of ether-type polar lipids in archaea and evolutionary
692 considerations. Microbiol Mol Biol Rev. 2007;71(1):97–120.
693 65. Hahn S, Stoilov IL, Tam Ha TB, Raederstorff D, Doss GA, Li HT, et al. Biosynthetic
694 studies of marine lipids. 17. The course of chain elongation and desaturation in long-
695 chain fatty acids of marine sponges. J Am Chem Soc. 1988;110(24):8117–24.
696 66. Barnathan G, Kornprobst JM, Doumenq P, Miralles J. New unsaturated long-chain
697 fatty acids in the phospholipids from the Axinellida sponges *Trikentrion loeve* and
698 *Pseudaxinella cf. lunaecharta*. Lipids. 1996;31(2):193–200.
699 67. Hougaard L, Christophersen C, Nielsen PH, Klitgaard A, Tendal O. The chemical
700 composition of species of *Geodia*, *Isops and Stryphnus* (Choristida: Demospongia:
701 Porifera)-A comparative study with some taxonomical implications. Biochem Syst
702 Ecol. 1991;19(3):223–35.
703 68. Makarieva TN, Santalova Ie, Gorshkova IA, Dmitrenok AS, Guzii AG, Gorbach VI, et
704 al. A new cytotoxic fatty acid (5Z,9Z)-22-methyl-5,9-tetracosadienoic acid and the

sterols from the far Eastern sponge *Geodinella robusta*. Lipids. 2006;37(1):75–80.

69. Morales RW, Litchfield C. Incorporation of ^{14}C-Acetate into C26 Fatty Acids of the Marine Sponge *Microciona prolifera*. Lipids. 1977;12(7):570-76.

70. Walkup RD, Jamieson GC, Ratcliff MR, Djerassi C. Phospholipid studies of marine organisms: 2.[1] Phospholipids, phospholipid-bound fatty acids and free sterols of the sponge *Aplysina fistularis* (Pallas) forma *fulva* (Pallas) (=*Verongia thiona*)[2]. Isolation and structure elucidation of unprecedented branched. Lipids. 1981;16(9):631–46.

Supplementary information

S1 Fig. Mass spectra of DMDS conducts of C_{26} (a,b) and C_{28} (c,d) LCFA with $\Delta^{9,19}$ (a,c) and $\Delta^{11,21}$ (b,d) unsaturation

S1 Table. All fatty acid compositional data. This excel file contains fatty acid data (µg g DW^{-1} and relative abundance (%), in PL and TL) of individual specimens. The excel file also contains the fragments of Me-branched C_{16} and C_{18}, the relative positions of saturated (branched and linear) FAMEs in hydrogenated samples and the isotope data.

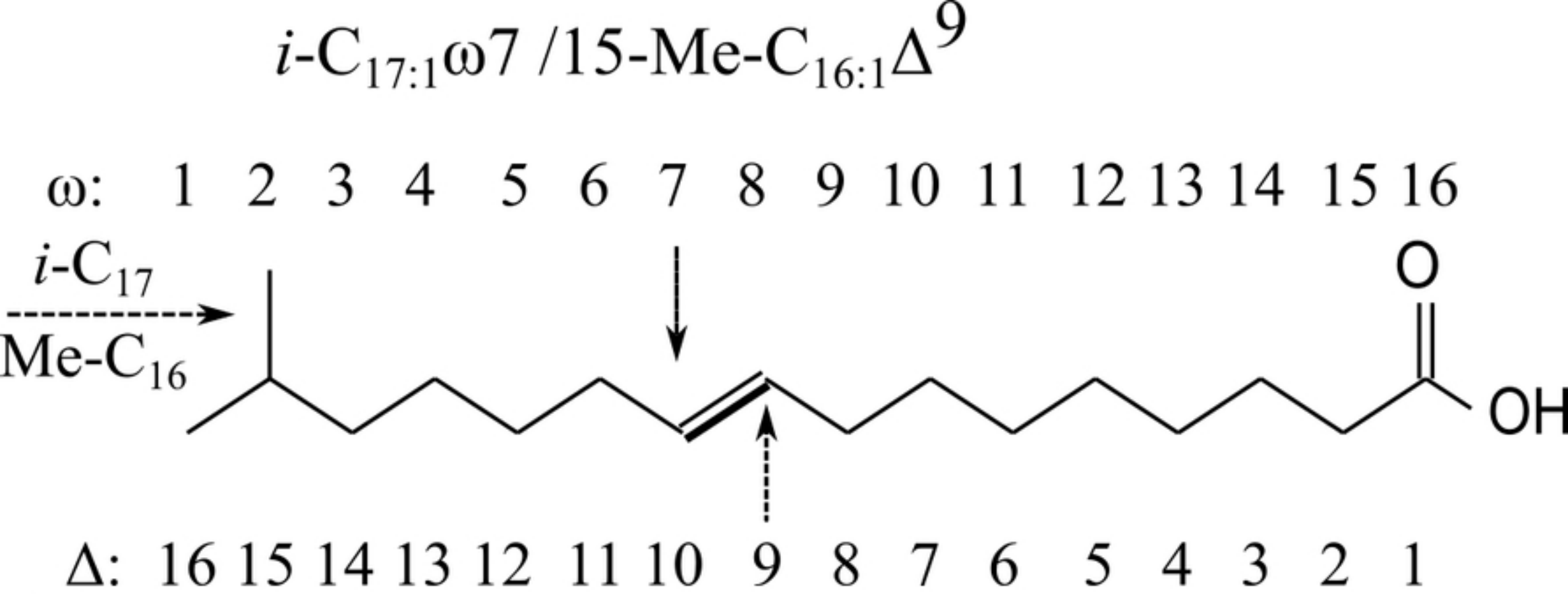
i-C17:1ω7 /15-Me-C16:1Δ9
ω: 1 2 3 4 5 6 7 8 9 10 11 12 13 14 15 16
i-C17
Me-C16
O
OH
Δ: 16 15 14 13 12 11 10 9 8 7 6 5 4 3 2 1

Figure 1

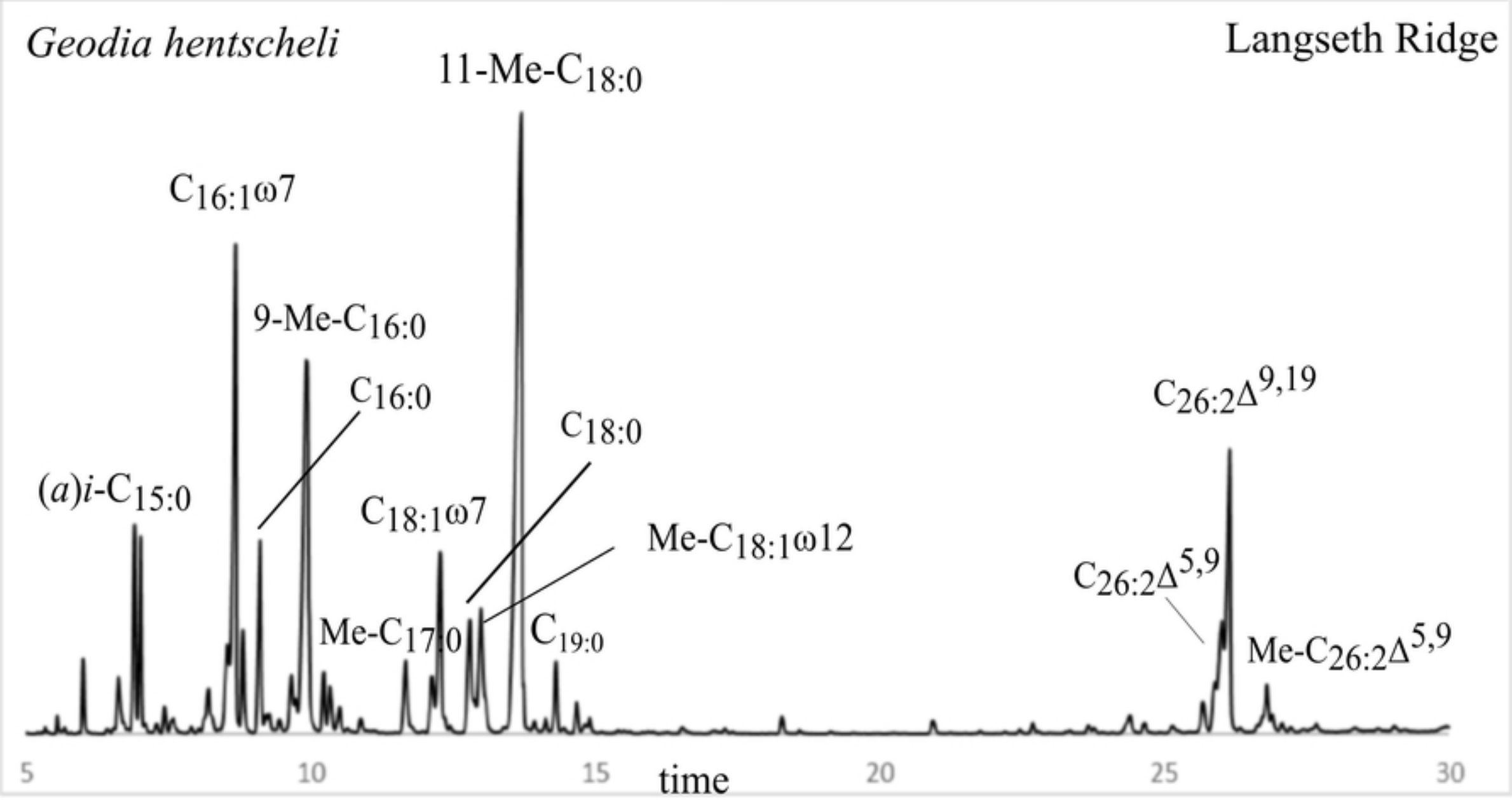
Geodia hentscheli
Langseth Ridge
11-Me-C18:0
C16:1ω7
9-Me-C16:0
C16:0
C18:0
(a)i-C15:0
C18:1ω7
Me-C18:1ω12
C26:2Δ9,19
C26:2Δ5,9
Me-C17:0
C19:0
Me-C26:2Δ5,9
5
10
15
time
20
25
30

Figure 2

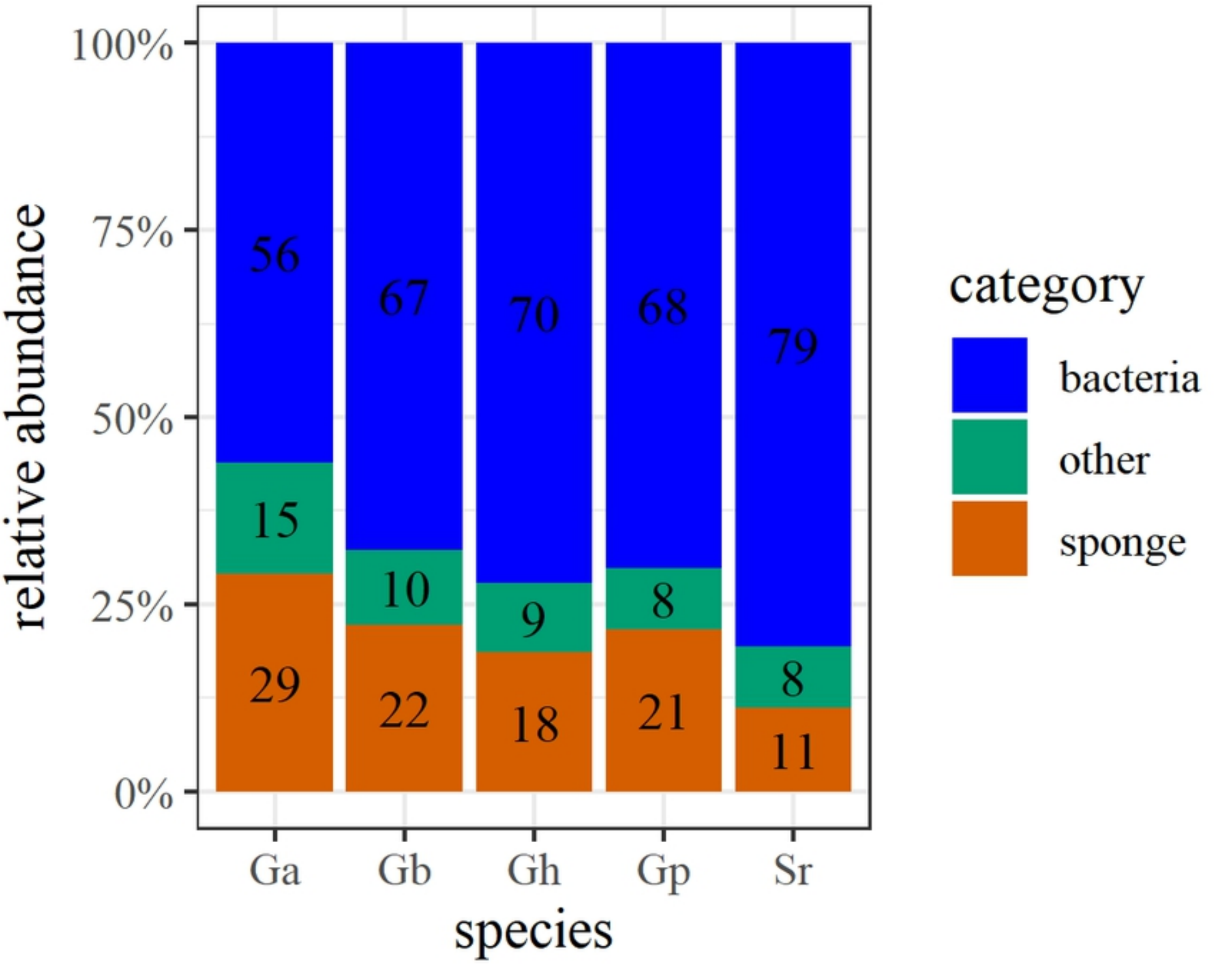
relative abundance
100%
75%
50%
25%
0%
56
67
70
68
79
15
10
9
8
8
29
22
18
21
11
Ga
Gb
Gh
Gp
Sr
species
category
bacteria
other
sponge

Figure 3

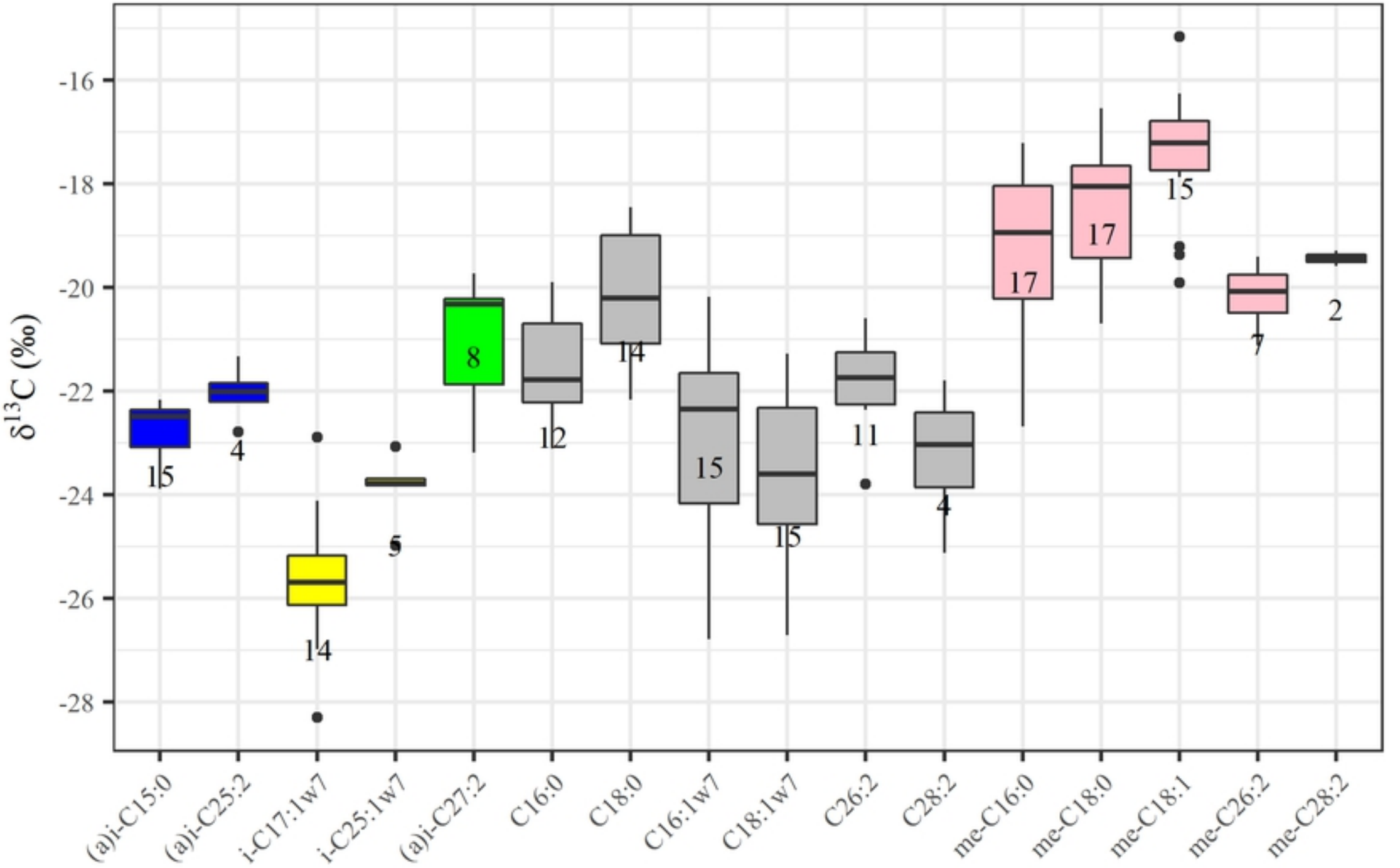
δ13C (‰)
-16
-18
-20
-22
-24
-26
-28
15
4
14
5
8
12
14
15
15
11
4
17
17
15
7
2
(a)i-C15:0
(a)i-C25:2
i-C17:1w7
i-C25:1w7
(a)i-C27:2
C16:0
C18:0
C16:1w7
C18:1w7
C26:2
C28:2
me-C16:0
me-C18:0
me-C18:1
me-C26:2
me-C28:2

Figure 4

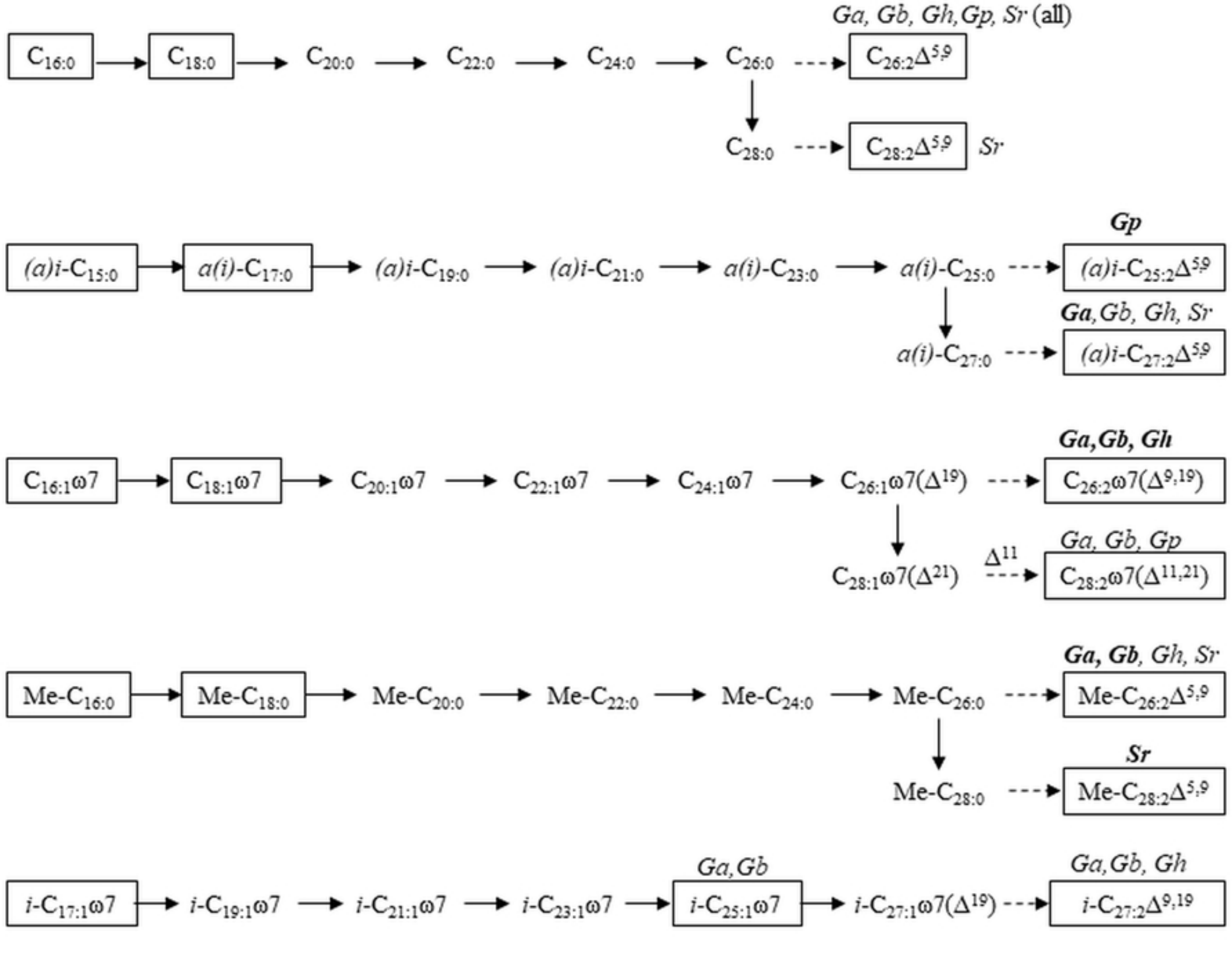
Ga, Gb, Gh,Gp, Sr (all)
C16:0
C18:0
C20:0
C22:0
C24:0
C26:0
C26:2Δ5,9
C28:0
C28:2Δ5,9
Sr
Gp
(a)i-C15:0
a(i)-C17:0
(a)i-C19:0
(a)i-C21:0
a(i)-C23:0
a(i)-C25:0
(a)i-C25:2Δ5,9
Ga,Gb, Gh, Sr
a(i)-C27:0
(a)i-C27:2Δ5,9
Ga,Gb, Gh
C16:1ω7
C18:1ω7
C20:1ω7
C22:1ω7
C24:1ω7
C26:1ω7(Δ19)
C26:2ω7(Δ9,19)
Ga, Gb, Gp
C28:1ω7(Δ21)
Δ11
C28:2ω7(Δ11,21)
Ga, Gb, Gh, Sr
Me-C16:0
Me-C18:0
Me-C20:0
Me-C22:0
Me-C24:0
Me-C26:0
Me-C26:2Δ5,9
Sr
Me-C28:0
Me-C28:2Δ5,9
Ga,Gb
Ga,Gb, Gh
i-C17:1ω7
i-C19:1ω7
i-C21:1ω7
i-C23:1ω7
i-C25:1ω7
i-C27:1ω7(Δ19)
i-C27:2Δ9,19

Figure 5